Journal of Composite Materials, vol. 33, no. 23,
pp. 2161-2192, 1999.

A Micromechanical Analysis of the Radial Elastic Response associated with Slender Reinforcing Elements within a Matrix

James V. Cox[1] and Hailing Yu
Department of Civil Engineering
Whiting School of Engineering
Johns Hopkins University
Baltimore, MD 21218

ABSTRACT: This paper addresses the elastic modulus associated with the radial interaction between a slender axisymmetric reinforcing element and a matrix. In particular, reinforcing elements with a significant surface structure are considered, and the elastic modulus of an interface model is defined to characterize the local elastic behavior resulting from the mechanical interaction that is not explicitly captured at a larger scale of modeling (i.e., a scale at which the surface structure is not explicitly modeled). An analytical justification for the elastic modulus is presented by determining the difference in the strain energy stored in a matrix that has a homogenized (or smoothed) interface traction distribution versus a more concentrated traction distribution that may occur with a complicated surface structure. Due to the importance of strain energy in driving cracks, it is postulated that the elastic modulus should be such that the composite with an idealized interface will store the same amount of strain energy as the actual composite having an interface with a surface structure. Analytical results show that the elastic modulus increases with the ratio of the contact area to the interface area and with a decrease in the period associated with a periodic traction distribution. A numerical example shows the effect of the elastic modulus on the prediction of longitudinal cracking in a quasibrittle matrix.*194 words*

Key words: surface structure, elastic moduli, homogenization, micromechanical, fiber, reinforcement, interface, interphase, imperfect interaction

James V. Cox: Dr. Cox is an assistant professor of Civil Engineering at Johns Hopkins University. His research interests are in modeling the mechanical behavior of materials and their interfaces and in computational mechanics. His recent work has focused on understanding and characterizing the mechanical interaction of steel and fiber-reinforced-polymer reinforcing elements with concrete. He completed his Ph.D. (under Professor L.R. Herrmann at U.C. Davis) in 1994.

[1] Correspondence author. Phone: (410) 516-6687

Hailing Yu: Ms. Yu is a Ph.D. student in the department of Civil Engineering at Johns Hopkins University. Her research focuses on understanding and characterizing the mechanical interaction along the interface of concrete and FRP/steel reinforcing elements.

1. INTRODUCTION

Interface descriptions of the mechanical interaction between two constituent materials of a body are common in computational mechanics. Often the characterization of this interaction includes an elastic component. For different applications the elastic component can be interpreted in various ways, e.g. representing: (1) the elastic behavior of a thin layer of the more compliant material (see e.g., Desai et al. [1]1984, and Desai and Nagaraj [2] 1986), (2) the elastic behavior of a thin interphase region (see e.g., Chaboche et al. [3]) that has different material properties than those of the constituent materials and is not otherwise represented in the model, (3) the local elastic response associated with omitted geometric detail of the surface structure (see e.g., Goodman et al. [4] 1968, and Herrmann [5] 1978, Plesha et al. [6] 1989, and Stankowski et al. [7]1993), and (4) a penalty parameter used to enforce a compatibility constraint (see e.g., Herrmann [5] 1978, and Oden and Campos [8] 1981). This last interpretation reflects that for some classes of problems the elastic moduli of the interface lack a physical interpretation.

This paper will focus on the third case, justification for elastic moduli when the interface has a *significant surface structure*[1]. Local response has been used to argue the need for elastic moduli associated with interface models, and reversible deformation of the contact zone has been experimentally measured for some applications (see e.g., Goodman et al. [4] 1968). However partially because the surface structure associated with many interface problems has a random structure (e.g., when the surface structure is associated with the roughness of an interfacial crack face), analytical results for elastic moduli appear to be lacking. This paper gives an analytical justification for an elastic modulus that characterizes average local behavior which is not explicitly captured at a larger scale (e.g., at a scale that might be used to model the matrix and reinforcing element numerically). We will examine a particular problem in which a slender axisymmetric reinforcing element can be idealized as (1) being stiff relative to the matrix and (2) having a periodic surface structure. While several simplifying assumptions are made for the analysis presented here, the general approach is applicable to a larger class of problems.

This study appears to be unique in: (1) its direct examination of the effects of a varying interface traction and (2) the characterization of the strain energy associated with the variation of the interface traction via the elastic modulus of an interface model. The study was motivated by computational modeling at a scale where the reinforcing element and matrix are modeled as solids; example computational analyses of composite materials at this scale include those of Chaboche et al. [3] Schellekens and de Borst [9], Tsai et al. [10] 1990, and Walter et al. [11]. Most studies on elastic moduli in composites having an interphase or imperfect interaction between the two phases have sought to determine the effective elastic moduli of an interphase region of finite thickness (see e.g., Ko et al. [12], and Navard and Keller [13]) or the effective elastic moduli of the complete composite (see e.g., Aboudi [14], Achenbach and Zhu [15], Benveniste [16], Hashin [17], Theocaris et al. [18], and the review of Jayaraman et al. [19]). In contrast, the elastic modulus (for an interface model) sought in this study was motivated by attempts to model failure of the mechanical interaction along an interface. While this paper

[1] *Surface structure* refers to the deviation of the actual geometry from that of the idealized model. For example, an idealized model might represent a reinforcing element as a circular cylinder. The surface structure in this case would be the portion of the actual reinforcing element that deviates from the idealized shape. The surface structure is referred to as being *significant* if it can produce significant mechanical interaction when forces occur along the interface.

addresses the radial (normal) component of the elastic interaction, the approach presented could also be used to examine the increased tangent compliance along a material interface due to imperfect interaction.

The physical problem that motivated this analytical study is that of the mechanical interaction between reinforcing bars (steel and fiber-reinforced-polymer[JVC1]) and a concrete matrix (Figure 1). These reinforcing elements have a fabricated surface structure (often idealized as being periodic) that can produce a complicated interface traction distribution, in part because of a reduction in the contact area after the propagation of an interfacial crack. Both physical and analytical evidence exists for the variation of interface tractions. Experimental studies (see e.g., Goto [20] and Jiang et al. [21]) have shown that local failure of the concrete initiates at the ribs on the surface of the bars. Numerical studies that explicitly model the surface structure (see e.g., Ozbolt and Eligehausen [22] and Reinhardt et al. [23]) have also demonstrated the concentration of tractions near the ribs on the bars. One scale of computational analysis for these types of problems (see e.g., Cox and Herrmann [24,25]) does not explicitly model the surface structure of the bar; rather the bar is modeled as a cylindrical solid. At this scale the effects of the local mechanical interaction must be accounted for indirectly, e.g., in an interface idealization. The same approach can be used for other composite materials in modeling the mechanics of misfit conditions arising from nonuniformity of the diameter of a reinforcing element (see e.g., [JVC2]Parthasarathy et al. [26]). This nonuniformity could be due to roughness that has a "characteristic wave length," (see e.g., reference) or a fabricated surface structure such as serrated fibers (see e.g., reference). However, there are many cases for which the effects of the "variation of the interface traction" are less likely to be of practical significance; e.g., the results presented later indicate that the effects of this variation decrease with a decrease in the "characteristic wave length."

When the surface structure of a reinforcing element is significant, the mechanical interaction associated with the corresponding misfit can be the most important contribution to the so called "*bond behavior*." Furthermore, this mechanical interaction can produce significant radial tractions at the interface (especially following the propagation of an interfacial crack). While experimental data (such as pull-out or push-out tests) may give an indication of the elastic response corresponding to the axial displacement of the reinforcing element, experimental data on the radial elastic response is often lacking; yet the radial elastic response can be important in computational predictions of composite behavior. For example, with reinforced concrete the radial traction component developed between the bars and concrete can produce longitudinal cracking that fails the system (see e.g., Tepfers [27]1979, and Cox 1997). The need to further examine the radial response was apparent in some of the validation problems for a bond model developed by Cox and Herrmann [28,25]. A preliminary study [29](Cox 1996) investigated the potential of including elastoplastic coupling in a bond model to account for the change in radial elastic response with differing contact conditions, but an analytical basis for the model was lacking. More recent applications of the model have addressed FRP reinforcement [30].

This paper focuses on the radial elastic response attributed to an interface idealization when the actual traction distribution along the interface is assumed to be axisymmetric and nonuniform (but periodic) in the axial direction. While the actual traction distribution will not generally satisfy these assumptions, these idealizations of the actual problem can allow analytical results to be obtained that yield significant insight. Furthermore, the analytical solution can be applied as a first order approximation when these assumptions are not strictly true.[JVC3]

The paper is organized as follows: the first section presents the simplifications that lead to the underlying analytical model; the second section presents the analytical solution; the third section shows how the analytical solution may be used to determine an equivalent elastic modulus of the interface idealization and presents analytical and numerical results; the fourth section presents an example to demonstrate the effect of the model on predicting longitudinal cracking in a quasibrittle matrix; and the fifth section presents a brief discussion and conclusions. The

emphasis of the paper is upon determining an analytical expression for the elastic modulus of the interface model.

2. ANALYTICAL MODEL

The interface idealization of bond can be described in terms of two simplifications. The first is the homogenization of the interface traction distribution and the simplification of the interface geometry. Figure 2 presents close-up views of sections (constant q) from an axisymmetric surface structure and the corresponding idealization that eliminates the detail of the surface structure. A cylindrical coordinate system is assumed with the z-axis corresponding to the axis of the bar. Figure 2a presents a schematic of the radial component of the interface traction (shown on the matrix) between the reinforcing element and the matrix for a *unit surface element*. The unit surface element consists of the complete interface surface for one cycle of the surface structure. The length of the unit surface element is denoted by s_r. Figure 2b presents a schematic of the normal component (shown negative) of the interface traction between the reinforcing element and matrix for the interface idealization. The interface idealization will yield a continuous traction distribution, that is smoother than the actual traction distribution. For example, the uniform distribution of s shown in Figure 2b (the "macroscopically homogeneous" case) would be the interface idealization of a periodic traction distribution as depicted in Figure 2a for a single interval. In conjunction with the simplification of the traction distribution, the actual surface geometry is also idealized as a cylindrical surface. Though not depicted in Figure 2, the actual interface geometry can change with material damage. In general, the homogenized stress is defined so that the average of each traction component in a cylindrical coordinate system is the same; for example

$$2\pi r\int_0^{s_r} s\,(z)dz = -\int_A T_r(z,q)dA \tag{1}$$

where A denotes the actual area of the unit surface element, and T_r denotes the radial component of the actual interface traction. As previously discussed, for the idealized problem considered here T_r is assumed to be axisymmetric and periodic; thus T_r is only a function of z, and s is uniform.

The second simplification, unique to interface idealizations, addresses the kinematics of a unit cell of the matrix adjacent to the interface (sometimes called the *bond zone*). Figures 2c and 2d give schematics of the deformation of the actual unit cell versus the deformation of the same unit cell for the interface model (again depicted for the "macroscopically homogeneous" case). d_n denotes the elastic extension of the interface (Figure 2d denotes a negative value), and D^e is the corresponding elastic modulus which satisfies

$$s = D^e d_n \tag{2}$$

point-wise. For the two unit cells, note the difference in the distribution of the radial displacement. The elimination of the surface structure and the corresponding traction concentrations – the first simplification – produce a different response in the matrix, even for a "perfect matrix model." While inelastic response can still occur with the interface idealization, the omission of the surface structure (which results in a less concentrated traction distribution) is likely to initially produce less inelastic response that is more distributed in the z-direction.

Now consider the idealizations that define the problem that will be solved analytically. The actual problem might have a geometry as depicted in Figure 2c. We adopt a cylindrical idealization of the surface geometry and project the actual tractions onto the cylindrical surface (accounting for the change in area). Furthermore, we assume: (1) a macroscopically homogeneous traction state (i.e., s is uniform), and (2) that the corresponding actual tractions vary periodically over the length of the unit surface element (s_r) and are evenly (or symmetrically) distributed about the center of each unit surface element. Boundary conditions are assumed such that we can consider the behavior of a single unit cell of a cylindrical domain as depicted in Figure 3. (Alternative boundary conditions will be discussed later.)

For *problem a* the elastic properties of the unit cell (**C**') are the effective elastic properties that include the effects of microcracks developed during loading, which would generally produce an inhomogeneous and anisotropic elastic solid at the mesoscale. (Even this rather general idealization includes the constraint that the spatial distribution of the material properties are symmetric about the center of the cell.) For the next level of idealization, *problem b*, the elastic properties are assumed to be homogeneous and isotropic. An "auxiliary problem," to either *problem a* or *b*, is defined in Figure 3c, where

$$\int_{-s_r/2}^{s_r/2} t_n dz = \tilde{t}_n \tilde{L}_t \tag{3}$$

(i.e., the tractions are said to be "statically equivalent") but an additional measure of "problem equivalence" must still be defined. $\tilde{t}_n$ and $\tilde{L}_t$ are the *equivalent traction* and *contact length*, respectively. (After we fully define "problem equivalence", it will be clear that the values of $\tilde{t}_n$ and $\tilde{L}_t$ would differ for "equivalent" auxiliary problems to *problems a* and *b*.) In concept *problem a* is closest to the actual problem, but effects of microcracking in the matrix are not considered in this study. The effect of the traction distribution will be considered, but since it is generally unknown it is usually sufficient to consider *problem c*. By proper definition of the elastic modulus, the interface idealization depicted in Figure 3d will also be an "equivalent auxiliary problem." In this case we have that

$$s s_r = \tilde{t}_n \tilde{L}_t \tag{4}$$

We will now consider measures of equivalence for the auxiliary problems. By Equations (3) and (4) *problems b*, *c*, and *d* are equivalent in a Saint-Venant sense (see e.g., Sokolnikoff [31]1956), assuming that for *problem d* $D^e \to \infty$ (i.e., when the elastic interface model is omitted). This measure of equivalence does not uniquely define $\tilde{t}_n$ and $\tilde{L}_t$. (This first measure of problem equivalence is analogous to defining macroscopic stresses in terms of volume averages in a continuum.) and it can not address how *problems a* and *d* could be "equivalent," since the two domains do not have the same material properties. An additional measure of "problem equivalence" (beyond "static equivalence" of the tractions) is needed. In particular, we seek to equate some measure of the response of the two models. For example, we first considered models that would have the same average radial displacement along the interface. It is a fairly simple exercise (see Appendix A) to show that the average radial displacements of *problems b, c* and *d* are the same when $D^e \to \infty$. However, the additional measure of "problem equivalence" should address the physical aspects of the problem that are important to retain with the homogenization of the interface tractions. As previously noted, in some cases the elastic response is very important in bond models toward the accurate prediction of matrix or interface cracking. Since the elastic energy stored in the material can be released to drive cracks, we will define the additional measure of "problem equivalence" as: two "equivalent problems" will store the same amounts of elastic strain energy in their domains. Thus the key to determining D^e is the solution of *problems b* through *d*. If we solve *problem b*, we can obtain an analytical solution for the elastic modulus and examine its dependence upon the traction distribution. (This second measure of problem equivalence is analogous to using energy-based approaches to determine effective elastic moduli of a continuum (or their bounds), but in this case the "effects are lumped to the interface.")

Focusing on the elastic response of the matrix to determine the elastic modulus associated with the mechanical interaction neglects the strain energy of the reinforcement. That is, "statically equivalent" traction distributions will also result in different amounts of strain energy stored in the reinforcing element. Thus, the following theoretical development is applicable when the elastic modulus of the reinforcement is much larger than that of the matrix; otherwise, it only presents half of the solution, since the solution for the reinforcement subjected to a periodic

normal traction should also be included.* Furthermore, the surface structures of some reinforcements could undergo significant deformation not accounted for in the solution presented here.

Determination of the effective elastic modulus of the interface has similarities with continuum damage mechanics which provides a mesoscopic description of the mechanical behavior of a microcracked solid. A simple definition of damage in a solid for the one-dimensional case is the effective surface density of microdefects (see e.g., Lemaitre [32]1992). One can view the change in elastic behavior attributed to an interface surface in a similar manner. Note that $\tilde{t}_n$ and $\tilde{L}_t$ are analogous to the *effective stress* and *effective area* of continuum damage mechanics for a solid [33](Kachanov 1958), and in an analogous manner generally $\tilde{L}_t \neq L_t$ – the difference in the general case being due to local damage of the matrix and the distribution of traction. Furthermore the relationship between the effective stress and homogenized stress (s) can be written as

$$\tilde{t}_n = \frac{s}{1-D} \tag{5a}$$

where

$$D = 1 - \frac{\tilde{L}_t}{s_r} \tag{5b}$$

Rather than postulating the applicability of a principle such as the strain equivalence principle [34](Lemaitre 1971)[JVC4], we will analytically determine how the elastic modulus varies with D by maintaining the same amount of elastic strain energy that exists with the "actual traction distribution." (For this problem, it is more natural to express the solution in terms of the fraction of the surface in contact, $\tilde{L}_t/s_r=1-D$.)

3. ANALYTICAL SOLUTION

3.1 Governing Equations

The governing equations for the axisymmetric problem are as follows. Equilibrium is governed by

$$\frac{\partial s_{rr}}{\partial r} + \frac{\partial s_{rz}}{\partial z} + \frac{s_{rr} - s_{qq}}{r} = 0, \qquad \frac{\partial s_{rz}}{\partial r} + \frac{\partial s_{zz}}{\partial z} + \frac{s_{rz}}{r} = 0, \tag{6a,b}$$

and $s_{ij}=s_{ji}$. The linear strain-displacement relationships are given by

$$e_{rr} = \frac{\partial u_r}{\partial r}, \qquad e_{qq} = \frac{u_r}{r}, \qquad e_{zz} = \frac{\partial u_z}{\partial z} \tag{7a,b,c}$$

$$e_{ra} = 0, \qquad e_{rz} = \frac{1}{2}\left(\frac{\partial u_z}{\partial r} + \frac{\partial u_r}{\partial z}\right), \qquad e_{az} = 0, \tag{7d,e,f}$$

and the constitutive relationship for linear isotropic elasticity can be written as

$$s_{rr} = l J + 2m e_{rr}, \quad s_{qq} = l J + 2m e_{qq}, \quad s_{zz} = l J + 2m e_{zz}, \quad s_{rz} = 2m e_{rz} \tag{8a-d}$$

where $J = e_{ii}$, and l and m are Lamé's constants. The boundary conditions are given by

$$u_z\big|_{z=-s_r/2} = u_z\big|_{z=s_r/2} = 0, \qquad s_{rz}\big|_{z=-s_r/2} = s_{rz}\big|_{z=s_r/2} = 0 \tag{9a,b}$$

$$s_{rr}\big|_{r=r_i} = t, \qquad s_{rz}\big|_{r=r_i} = 0 \tag{9c,d}$$

* The simpler case is shown here for brevity; effects of the deformation of the reinforcement will be presented in the dissertation work of the second author.

$$\sigma_{rr}\big|_{r=r_o} = 0, \qquad \sigma_{rz}\big|_{r=r_o} = 0 \tag{9e,f}$$

where t denotes a generic distribution of traction normal to the surface (i.e., it may represent either t_n or $\tilde{t}_n$).

3.2 Solution

Due in part to the symmetry of the problem defined over a unit cell, the solutions for u_r and u_z are even and odd functions of z, respectively. The solution will be obtained in a manner similar to the Levy solution for simply supported plates [35] (Timoshenko and Woinowsky-Krieger 1959).* The nonzero displacement components are written in terms of orthonormal bases for square integrable even and odd functions of z as

$$u_r(r,z) = \sum_{n=0}^{\infty} \nu_{rn}(r)F_{cn}(z), \qquad u_z(r,z) = \sum_{n=1}^{\infty} \nu_{zn}(r)F_{sn}(z) \tag{10a,b}$$

where

$$F_{cn}(z) = \begin{cases} \dfrac{1}{\sqrt{\sigma_r}}, & n=0 \\ \dfrac{\cos(z\omega_n)}{\sqrt{\sigma_r/2}}, & n>0 \end{cases}, \qquad F_{sn}(z) = \frac{\sin(z\omega_n)}{\sqrt{\sigma_r/2}}, \qquad \omega_n = \frac{2\pi n}{\sigma_r} \tag{10c-e}$$

Since these are orthonormal bases for the variation of the functions in z for a fixed r, the coefficient functions are just projections of the solution onto each basis function, i.e.,

$$\nu_{rn}(r) = \langle u_r(r,z), F_{cn}(z)\rangle, \qquad \nu_{zn}(r) = \langle u_z(r,z), F_{sn}(z)\rangle \tag{11a,b}$$

where $\langle a,b\rangle = \int_{-\sigma_r/2}^{\sigma_r/2} ab\,dz$. These coefficient functions can be found by projecting the governing equations onto the basis functions. For the equilibrium equations this can be written as

$$\left\langle F_{cn}, \frac{\partial \sigma_{rr}}{\partial r} + \frac{\partial \sigma_{rz}}{\partial z} + \frac{\sigma_{rr}-\sigma_{\theta\theta}}{r} \right\rangle = 0, \qquad \left\langle F_{cn}, \frac{\partial \sigma_{rz}}{\partial r} + \frac{\partial \sigma_{zz}}{\partial z} + \frac{\sigma_{rz}}{r} \right\rangle = 0 \tag{12a,b}$$

$$\left\langle F_{sn}, \frac{\partial \sigma_{rr}}{\partial r} + \frac{\partial \sigma_{rz}}{\partial z} + \frac{\sigma_{rr}-\sigma_{\theta\theta}}{r} \right\rangle = 0, \qquad \left\langle F_{sn}, \frac{\partial \sigma_{rz}}{\partial r} + \frac{\partial \sigma_{zz}}{\partial z} + \frac{\sigma_{rz}}{r} \right\rangle = 0 \tag{12c,d}$$

The left sides of Equations (12b) and (12c) are identically zero since in both cases one factor in the inner product is an odd function and the other factor is an even function of z. Substituting the constitutive Equations (8) and strain-displacement relationships (7) into Equations (12a) and (12d) gives two equations for the displacement components (for $n>0$). Then using the orthonormality of the bases and Equations (11), we obtain the following set of coupled ordinary differential equations for ν_{rn} and ν_{zn} ($n>0$)

$$-\nu_{rn}\left(\mu\omega_n^2 + \frac{\alpha}{r^2}\right) + \frac{d\nu_{rn}}{dr}\left(\frac{\alpha}{r}\right) + \frac{d^2\nu_{rn}}{dr^2}(\alpha) + \frac{d\nu_{zn}}{dr}(\beta\omega_n) = 0$$

$$-\nu_{rn}\left(\frac{\beta\omega_n}{r}\right) - \frac{d\nu_{rn}}{dr}(\beta\omega_n) - \nu_{zn}(\alpha\omega_n^2) + \frac{d\nu_{zn}}{dr}\left(\frac{\mu}{r}\right) + \frac{d^2\nu_{zn}}{dr^2}(\mu) = 0 \tag{13a,b}$$

where $\alpha = \lambda+2\mu$ and $\beta = \lambda+\mu$. By the same methodology, for the case of $n=0$, Equation (12a) gives

---

* A related numerical solution for a ring stiffened shell rocket booster was previously given by Herrmann and Tamekuni [36]1965. Kurtz and Pagano [37] used stress functions to examine the deformation of a fiber within a matrix and referenced several analytical solutions using the same approach to solve related problems.

$$\frac{d^2 n_{r0}}{dr^2} + \frac{1}{r}\frac{dn_{r0}}{dr} - \frac{n_{r0}}{r^2} = 0 \tag{14}$$

Taking the derivative of Equation (13b), multiplying it by $a/(bw_n)$, and adding it to Equation (13a), gives the following relationship for n_{rn}

$$n_{rn} = \frac{a}{bw_n^3}\left(\frac{d^3 n_{zn}}{dr^3} + \frac{1}{r}\frac{d^2 n_{zn}}{dr^2} - \frac{1}{r^2}\frac{dn_{zn}}{dr}\right) - \left(\frac{a+b}{bw_n}\right)\frac{dn_{zn}}{dr} \tag{15}$$

Substituting this into Equation (13b) gives a fourth order ordinary differential equation that can be shown to be of the form

$$L_n(L_n(v_{zn})) = 0 \tag{16}$$

where L_n is the differential operator given by

$$L_n = \frac{d^2}{dr^2} + \frac{1}{r}\frac{d}{dr} - w_n^2 \tag{16b}$$

The change of variables $y=w_n r$ allows L_n to be expressed as the modified Bessel operator of order 0:

$$L_n = y^2\frac{d^2}{dy^2} + y\frac{d}{dy} - y^2 \tag{17}$$

(The dependence of L_n upon n is not explicitly shown since it enters through the definition of y.) By employing the following properties of the modified Bessel functions of the first and second kinds:

$$L_n\left[I_0(y)\right] = 0, \quad L_n\left[K_0(y)\right] = 0, \quad L_n\left[yI_1(y)\right] = 2w_n^2 I_0(y), \quad L_n\left[yK_1(y)\right] = -2w_n^2 K_0(y)$$

the solution of each coefficient function can be expressed in the form

$$v_{r0}(r) = c_{10}r + c_{20}\frac{1}{r} \tag{18a}$$

$$v_{rn}(r) = -c_{1n}I_1(w_n r) + c_{2n}K_1(w_n r) + c_{3n}\left[4(1-n)I_1(w_n r) - w_n r I_0(w_n r)\right] + c_{4n}\left[4(1-n)K_1(w_n r) + w_n r K_0(w_n r)\right] \tag{18b}$$

$$v_{zn}(r) = c_{1n}I_0(w_n r) + c_{2n}K_0(w_n r) + c_{3n}w_n r I_1(w_n r) + c_{4n}w_n r K_1(w_n r) \tag{18c}$$

Now with the general form of the solution for the displacements, the solution for the stress field can be obtained. For this study, only the s_{rr} and s_{rz} components are needed to address the boundary conditions and to determine D^e. Combining the strain-displacement relations (7), the constitutive Equations (8), and solution for the displacements (10, 18), the stress components can be expressed as

$$s_{rr} = \sum_{n=0}^{\infty} s_n(r)\Phi_{cn}(z), \qquad s_{rz} = \sum_{n=1}^{\infty} t_n(r)\Phi_{sn}(z) \tag{19a,b}$$

where

$$s_0(r) = s_{c_{10}}c_{10} + s_{c_{20}}c_{20} \tag{20a}$$

$$s_n(r) = 2m\left(s_{c_{1n}}c_{1n} + s_{c_{2n}}c_{2n} + s_{c_{3n}}c_{3n} + s_{c_{4n}}c_{4n}\right) \tag{20b}$$

$$t_n(r) = 2m\left(t_{c_{1n}}c_{1n} + t_{c_{2n}}c_{2n} + t_{c_{3n}}c_{3n} + t_{c_{4n}}c_{4n}\right) \tag{20c}$$

and

$$s_{c_{10}} = 2(l+m), \qquad s_{c_{20}} = -2m/r^2 \tag{21a,b}$$

$$s_{c_{1n}} = -w_n I_0(w_n r) + I_1(w_n r)/r, \qquad s_{c_{2n}} = -w_n K_0(w_n r) - K_1(w_n r)/r \tag{21c,d}$$

$$s_{c_{3n}} = (3-2n)w_n I_0(w_n r) - 4(1-n)I_1(w_n r)/r - w_n^2 r I_1(w_n r) \tag{21e}$$

$$s_{c_{4n}} = -(3-2n)w_n K_0(w_n r) - 4(1-n)K_1(w_n r)/r - w_n^2 r K_1(w_n r) \quad (21f)$$

$$t_{c_{1n}} = w_n I_1(w_n r), \qquad t_{c_{2n}} = -w_n K_1(w_n r) \quad (22a,b)$$

$$t_{c_{3n}} = w_n^2 r I_0(w_n r) - 2(1-n)w_n I_1(w_n r) \quad (22c)$$

$$t_{c_{4n}} = -w_n^2 r K_0(w_n r) - 2(1-n)w_n K_1(w_n r) \quad (22d)$$

(For Equations (21c) through (22d), n>0.)

Projecting the boundary conditions (9c-f) and using Cauchy's relationship between traction and stress components gives the following Equations for the unknown coefficients

$$\langle \Phi_{cn}, s_{rr} \rangle\big|_{r=r_i} = \langle \Phi_{cn}, t \rangle \qquad \langle \Phi_{sn}, s_{rz} \rangle\big|_{r=r_i} = 0 \quad (23a,b)$$

$$\langle \Phi_{cn}, s_{rr} \rangle\big|_{r=r_o} = 0 \qquad \langle \Phi_{sn}, s_{rz} \rangle\big|_{r=r_o} = 0 \quad (23c,d)$$

Equations (19-22) and the properties of the basis functions allow these equations to be expressed as

$$\begin{bmatrix} s_{c_{10}}\big|_{r=r_i} & s_{c_{20}}\big|_{r=r_i} \\ s_{c_{10}}\big|_{r=r_o} & s_{c_{20}}\big|_{r=r_o} \end{bmatrix} \begin{Bmatrix} c_{10} \\ c_{20} \end{Bmatrix} = \begin{Bmatrix} a_0 \\ 0 \end{Bmatrix} \quad (24a)$$

$$\begin{bmatrix} s_{c_{1n}}\big|_{r=r_i} & s_{c_{2n}}\big|_{r=r_i} & s_{c_{3n}}\big|_{r=r_i} & s_{c_{4n}}\big|_{r=r_i} \\ s_{c_{1n}}\big|_{r=r_o} & s_{c_{2n}}\big|_{r=r_o} & s_{c_{3n}}\big|_{r=r_o} & s_{c_{4n}}\big|_{r=r_o} \\ t_{c_{1n}}\big|_{r=r_i} & t_{c_{2n}}\big|_{r=r_i} & t_{c_{3n}}\big|_{r=r_i} & t_{c_{4n}}\big|_{r=r_i} \\ t_{c_{1n}}\big|_{r=r_o} & t_{c_{2n}}\big|_{r=r_o} & t_{c_{3n}}\big|_{r=r_o} & t_{c_{4n}}\big|_{r=r_o} \end{bmatrix} \begin{Bmatrix} c_{1n} \\ c_{2n} \\ c_{3n} \\ c_{4n} \end{Bmatrix} = \begin{Bmatrix} a_n/(2m) \\ 0 \\ 0 \\ 0 \end{Bmatrix} \quad (24b)$$

where the a's are the coordinates of t in the F_c basis, i.e.,

$$a_n = \langle \Phi_{cn}, t \rangle \quad (25)$$

The solution of Equation (24a) gives

$$c_{10} = \frac{a_0 r_i^2}{2(l+m)(r_i^2 - r_o^2)} \qquad c_{20} = \frac{a_0 r_i^2 r_o^2}{2m(r_i^2 - r_o^2)} \quad (26a,b)$$

Solving Equation (24b) for each n>0 gives the remaining unknown coefficients, thus completing the solution for both the displacement and stress fields. While the exact solution to this linear system of equations can be expressed analytically, the expression is omitted for brevity.

3.3 Verification

The mathematical correctness of the above solution was evaluated using symbolic manipulation and by examining the predicted solution for three problems. The first problem simply verified that the solution reduces to the classical solution for a thick-walled cylinder subjected to a uniform traction over the unit cell. For this case t is proportional to F_{c0} thus a_n=0 for all n>0. The solution then follows directly from Equations (26).

In the second problem, we examine the form of the solution for an arbitrary t when $r_o \to \infty$. The properties of the modified Bessel functions of the first and second kind imply that as $r \to \infty$ $s_{c_{1n}}, s_{c_{3n}}, t_{c_{1n}}, t_{c_{3n}} \to \infty$ and $s_{c_{2n}}, s_{c_{4n}}, t_{c_{2n}}, t_{c_{4n}} \to 0$, respectively. Thus, by Equations (24), bounding the solution "at infinity" implies that c_{1n}= c_{3n} =0 for all n. Equations (24) then reduce to

$$\left(s_{c_{20}}\big|_{r=r_i}\right) c_{20} = a_0 \quad (27a)$$

$$\begin{bmatrix} s_{c_{2n}}\big|_{r=r_i} & s_{c_{4n}}\big|_{r=r_i} \\ t_{c_{2n}}\big|_{r=r_i} & t_{c_{4n}}\big|_{r=r_i} \end{bmatrix} \begin{Bmatrix} c_{2n} \\ c_{4n} \end{Bmatrix} = \begin{Bmatrix} a_n/(2m) \\ 0 \end{Bmatrix} \tag{27b}$$

for which the solution is given by

$$c_{20} = \frac{-a_0 r_i^2}{2m} \tag{28a}$$

$$c_{2n} = \frac{a_n r_i \left[-w_n r_i K_0(w_n r_i) - 2(1-n)K_1(w_n r_i)\right]}{2mA(w_n r_i)} \qquad n>0 \tag{28b}$$

$$c_{4n} = \frac{a_n r_i K_1(w_n r_i)}{2mA(w_n r_i)} \qquad n>0 \tag{28c}$$

where

$$A(w_n r_i) = w_n^2 r_i^2 \left[K_0^2(w_n r_i) - K_1^2(w_n r_i)\right] - 2(1-n)K_1^2(w_n r_i) \tag{29}$$

The coefficient functions for the displacement and stress components (n>0) are then given by

$$v_{rn}(r) = \frac{a_n r_i \left[-w_n r_i K_0(w_n r_i)K_1(w_n r) + w_n r K_1(w_n r_i)K_0(w_n r) + 2(1-n)K_1(w_n r_i)K_1(w_n r)\right]}{2mA(w_n r_i)} \tag{30a}$$

$$v_{zn}(r) = \frac{a_n r_i \left[-w_n r_i K_0(w_n r_i)K_0(w_n r) + w_n r K_1(w_n r_i)K_1(w_n r) - 2(1-n)K_1(w_n r_i)K_0(w_n r)\right]}{2mA(w_n r_i)} \tag{30b}$$

$$\begin{aligned} s_n(r) = a_n w_n r_i \big[& w_n r_i K_0(w_n r_i)K_0(w_n r) + r_i K_0(w_n r_i)K_1(w_n r)/r - K_1(w_n r_i)K_0(w_n r) \\ & -2(1-n)K_1(w_n r_i)K_1(w_n r)/(w_n r) - w_n r K_1(w_n r_i)K_1(w_n r)\big] \Big/ A(w_n r_i) \end{aligned} \tag{30c}$$

$$t_n(r) = \frac{a_n w_n r_i \left[w_n r_i K_0(w_n r_i)K_1(w_n r) - w_n r K_1(w_n r_i)K_0(w_n r)\right]}{A(w_n r_i)} \tag{30d}$$

While these results were derived for an infinite domain, they are also useful for obtaining accurate approximations of finite domain problems. Application of the general solution previously derived for finite domains, requires the solution of Equation (24b) for each n>0. While all of the terms of the matrix remain bounded for a finite domain, the difference in the asymptotic behavior of modified Bessel functions of the first and second kinds can result in coefficients which vary by many orders of magnitude (e.g., differing by a factor of 10^{-10}) – the smaller coefficients being those multiplied by terms that include modified Bessel functions of the first kind. Even the associated product terms (e.g., $s_{c_{1n}} c_{1n}$) can be many orders of magnitude smaller (e.g., differing by a factor of 10^{-6}) than those associated with modified Bessel functions of the second kind. The dominance of the terms associated with functions of the second kind increases with n and r_o/r_i, and tends to result in increasingly ill-conditioned linear systems of equations. Thus for the problems that motivated this study ($r_o/r_i \geq 4$), the solution for infinite domains is accurate for n>0. (This observation will be further demonstrated in the next section.) *Hailing verify all of this. Hailing didn't feel this detail was necessary, but without it I'm concerned that equations (24 may be misapplied.*

The last verification problem compares numerical results obtained from the above solution to those obtained from a finite element (FE) analysis of a unit cell. The unit cell corresponds to a concrete bond specimen [38] Malvar (1992) with the following properties: r_i = 9.525 mm, r_o =4 r_i, L_t=1.587 mm, s_r=12.8 mm, E=38700 MPa, and n=0.17. The normal traction is uniform with a magnitude of s_r/L_t MPa (i.e. corresponds to σ=1 MPa).

Figure 4 shows the comparison of displacement components (u_r and u_z) along r and z coordinate directions for all of the solutions. Two solutions using the analytical expressions are shown to indicate the extent of convergence. The finite element solution used 392 bilinear quadrilateral elements graded more finely near the applied traction. While the finite element mesh is not sufficient to capture the [JVC5]discontinuity in e_{zz} near the edge of the load (Figure 4a), its overall agreement with the analytical solution suggests that the analytical solution is correct.

Figure 5 shows the FE predicted distribution of s_{rr} for one half of the unit cell. Clearly the difference in response between the actual and homogenized traction is very local; this behavior is consistent with the previous observation – that for n>0 (the terms associated with the local response) the solution is not sensitive to r_o for the problems that motivated this study. The extent of the local response also gives an indication of the minimum "fiber spacing" for which the analysis is applicable to. With an analytical solution, we can now return to the problem of determining an expression for the elastic modulus associated with the interface – a direct consequence of the local behavior.

4. ELASTIC MODULUS

4.1 Formulation

We previously defined *equivalent problems* as those that store the same amount of elastic energy and have "statically equivalent" traction distributions. The strain energy stored in an elastic unit cell is equal to the work done by the traction t. Therefore, we can simply use the analytical solution to compute the work done by the interface tractions in *problems b* and *d*, and then equate them to determine an expression for D^e. The work done by the tractions in *problem b* is given by

$$\begin{aligned} W_b &= -p r_i \int_{-s_r/2}^{s_r/2} t(z) u_r(r_i, z) dz \\ &= -p r_i \sum_{n=0}^{\infty} a_n n_{rn}(r_i) \end{aligned} \tag{31}$$

where the last relationship uses the expressions for both factors of the integrand in terms of the F_c basis and exploits the orthonormality of the basis. Using the definition of the elastic modulus (2), the work done by the tractions in *problem d* is given by

$$\begin{aligned} W_d &= (p r_i s_r) s \left[-u_r(r_i) + d_n \right] \\ &= (p r_i s_r) s \left[-u_r(r_i) + s / D^e \right] \end{aligned} \tag{32}$$

where, by Equations (11) and (3),

$$s = \frac{1}{s_r} \int_{-s_r/2}^{s_r/2} t(z) dz \tag{33}$$

(Note that the notation $u_r(r)$ unambiguously refers to the radial displacement for *problem d*, since the displacement for *problem b* also varies with z.) Equating the work in the two systems gives

$$D^e = \frac{s_r s^2}{s_r s u_r(r_i) - \sum_{n=0}^{\infty} a_n n_{rn}(r_i)} \tag{34}$$

By the definitions of s and F_{c0}, $a_0 = s\sqrt{s_r}$. Furthermore, as shown in Appendix A, the average radial displacement for "statically equivalent" traction distributions is the same. Thus, we also have the relationship that $n_{r0}(r_i) = u_r(r_i)\sqrt{s_r}$. The expression for the elastic modulus can be simplified to

$$D^e = \frac{s_r s^2}{-\sum_{n=1}^{\infty} a_n n_{rn}(r_i)} \tag{35}$$

Now let us examine the dependence of the elastic modulus upon Young's modulus (E) and the diameter of the reinforcing element (d_f). To do so, it will be convenient to express $n_{rn}(r_i)$ in the symbolic form – *note $w_n r_o$ was eliminated due to its linear dependence*

$$n_{rn}(r_i) = \frac{a_n r_i h(w_n r_i, r_i/r_o, n)}{E} \tag{36}$$

where h is a dimensionless function. This form follows from Equations (18-24); a simpler version of this form is readily apparent in the solution for the special case when $r_o \to \infty$, Equations (30a,c). The elastic modulus can now be expressed as

$$D^e = \frac{2E}{-d_f \sum_{n=1}^{\infty} \left(\frac{a_n}{a_0}\right)^2 h(w_n r_i, r_i/r_o, n)} \tag{37}$$

where d_f denotes the diameter of the "fiber" ($2r_i$). Assume that the geometry of the surface structure scales with d_f. Furthermore, assume that (for a given load level) the scaling of the surface structure geometry will scale the traction distribution accordingly. Then both a_n/a_0 and $w_n r_i$ are independent of d_f. If r_o is sufficiently larger than the range of r_i to be considered (i.e., the solution for the infinite domain case is sufficiently accurate), then D^e is inversely proportional to the diameter of the reinforcing element. As expected the elastic modulus varies proportionately with Young's modulus of the matrix, but the variation with Poisson's ratio is complicated.

The denominator of Equation (37) gives a direct measure of the effect of having a nonuniform traction distribution. As previously noted, the zero terms of Equations (10a) and (19a) give the response of the unit cell for a uniform traction distribution. All of the other terms in the series expansions account for the deviation from a uniform distribution. Furthermore, the orthonormality of the basis functions implies that the contributions of the other terms ($n>0$) correspond to traction components that are "statically equivalent to a zero traction." Thus in a Saint-Venant sense, these other terms represent the local response.

Alternative boundary conditions to those defined by Equations (9) (Figure 3) could also be considered. One alternative is to allow the unit cell to exhibit uniform axial displacement along the sides ($z=\pm s_r/2$). It can be shown by superposition that while the solution of the boundary value problem differs, the value for the elastic modulus does not change. A second alternative is to include a normal traction on the outer surface (σ_o) of the unit cell ($r=r_o$). For this case, Equations (31) and (32) must include the work done by σ_o. Using reciprocity and superposition one can show that if σ_o is a constant, then again the elastic modulus is the same as that calculated from the original boundary conditions; when σ_o is not a constant, Saint-Venant's principle indicates that the effect of σ_o upon D^e will decrease with an increase in r_o. (The effects of r_o are considered in the subsection below.)

Generally the interface traction distribution is an unknown, but the emphasis here is not upon the direct application of Equation (37). In some cases (e.g., if one could estimate a contact area based upon a known surface structure) one could use Equation (37) to estimate D^e for an analysis where it would be treated as a constant. As previously discussed there is also motivation in some applications to consider the effects of changing contact conditions on the elastic response even

though there are also several uncertainties. The analysis does provide qualitative insight on the effects of imperfect contact conditions. We will briefly consider factors that affect the elastic modulus, including: (1) contact length, (2) traction distribution, and (3) unit cell length (s_r).

4.2 Results

Most of the following results are presented in a nondimensional form and thus are not tied to a particular application. The parameters that define the problem are given by: r_o/r_i =4, s_r/r_i =1.34, and n=0.17 (unless indicated otherwise).

Figure 6 shows the variation of the elastic modulus with respect to contact length and for two different traction distributions over L_t (uniform and cosine). (Over the contact length, the cosine distribution is given by $t(z)=t_{max}cos(z\pi/L_t)$, where t_{max} denotes the maximum traction value.) These analytical results support the postulate[JVC6] that the compliance of the interface should increase with a reduction in the contact length. The results also indicate that the effect of the traction distribution decreases with the contact length. As previously noted, since both the contact length and traction distribution are unknown it may be simpler to consider an equivalent system that has a uniform traction distribution over the effective contact length. Equivalent systems will store the same amounts of elastic strain energy, and thus will have the same elastic modulus. As an example (see the "box" on Figure 6), a cosine distribution with a contact length of $s_r/2$ will have an equivalent contact length of about $0.38s_r$, which is intuitively consistent with the cosine distribution being more concentrated (for a fixed L_t) than a uniform distribution associated with the same "radial force."

For the uniform traction distribution over the contact length, $D^e \rightarrow \infty$ as $L_t \rightarrow s_r$, since *problems c* and *d* are the same under these conditions. In contrast, for the cosine traction distribution D^e approaches a constant value for full-contact conditions. That is, even if full contact exists along the interface, any homogenization of a nonuniform traction distribution requires a finite elastic modulus for the interface if the two systems are to store the same amount of elastic strain energy. Also note that the effective contact length has a length less than the unit surface element.

To incorporate the dependence of D^e upon the effective contact length into a bond model requires the contact length to be related to other variables in the model. These relationships may include the effects of local material damage upon the effective contact area; thus they are application specific, and not within the scope of this study. (A model that relates the contact length to other model variables was recently combined with the analytical results presented here [39][Cox and Yu 1998] in the context of concrete modeling and significantly improved the radial response of a bond model.)

Figures 7 through 10 examine the effects of some of the other parameters upon the elastic modulus of the interface. Figure 7 shows the relative insensitivity of the solution to Poisson's ratio. Figure 8 shows that for this case the infinite domain solution is relatively accurate for $r_o/r_i>2$, suggesting that it is "applicable" when the reinforcement is separated by a distance of d_f. Figure 9 shows the variation of the elastic modulus with respect to changes in both s_r and L_t. The intersect of the two curves corresponds to the last verification problem (results shown in Figure 5). For the parameters of this problem, D^e is more sensitive to a change in s_r/L_t due to a change in s_r than due to a change in L_t. Figure 10 indicates how D^e varies with respect to s_r for fixed values of s_r/L_t. Clearly the elastic modulus depends upon the fractional contact area and upon the length of the unit surface element – a characteristic length associated with the surface structure.

5. EXAMPLE APPLICATION

Now consider the application of the elastic modulus to a problem that includes longitudinal cracking. The derivation of D^e was based upon an axisymmetric problem, yet the motivation for this study was to correctly characterize the strain energy stored in a matrix when the problem is modeled at a scale in which the details of the traction distribution have been homogenized – in

particular to characterize the strain energy available for driving longitudinal cracking in the matrix.

For demonstration, we again examine a concrete bond specimen [38]. In the actual bond experiments, the radial components of the interface traction result from a complex mechanical interaction, but the effects of the elastic modulus can be demonstrated with a simpler problem. The specimen is subjected to radial interface tractions corresponding to the macroscopic homogenous traction case. Four axisymmetric finite element models of the specimen are adopted with different idealizations.

In all four models a simplified representation of the longitudinal cracking in concrete is adopted; this type of representation originated with the analytical work of Tepfers [27]. The model presented here (for a FEM analysis) follows the approach of Rots [40], where the effects of longitudinal cracking are incorporated into an "axisymmetric material model." Figure 11 shows the end-view of a specimen having three longitudinal cracks. Each crack is idealized as being planar with a process zone of infinitesimal thickness, and all of the cracks are assumed to grow concurrently. The process zone in the plane of the crack has a finite length and is referred to as the *cohesive crack* [41](Hillerborg *et al.* [1976]). The nonlinear behavior of the process zone is characterized by the following traction–crack opening relationship for the cohesive crack

$$s_{cr} = f_t\left[\left(1+c_1\hat{w}^3\right)e^{-c_2\hat{w}} - \left(1+c_1\right)\hat{w}e^{-c_2}\right] \tag{38}$$

where $\hat{w}$ is the ratio of the opening displacement of the cohesive crack and the minimum crack opening (w_o) for which there is no traction across the crack, f_t is the tensile strength of the concrete, and c_1 and c_2 are model parameters. For this example, we assume three longitudinal cracks can develop, f_t=4.69 MPa, w_o=0.11 mm, c_2=6.93, and c_1 is selected so that the energy required to create additional crack surface (the so called *fracture energy*) is 100 J/m^2 – a typical value for normal strength concrete. This relationship is graphically depicted in Figure 12.

To incorporate the effects of longitudinal cracking in the context of an axisymmetric model the hoop response of the "material model" is modified. The matrix material between the longitudinal cracks is assumed to be linear elastic (E=38700 MPa and n=0.17) and in an axisymmetric stress state; *i.e.*, the hoop stress is assumed to be independent of q and equal to the traction across the cohesive crack. The sum of the crack openings associated with a given point (i.e., for fixed values of r and z) is divided by the circumference giving an additional contribution to the "effective hoop strain."

Four finite element models address different levels of idealization. Figure 13 depicts the most complex model – *model 1*. The actual material interface geometry is explicitly modeled, and uniform tractions are applied to inclined surfaces. *Model 2* omits the detail of the surface structure adopting a cylindrical representation (as Figure 3b), with uniform tractions applied over the same projected areas. *Models 3 and 4* represent the macroscopic idealizations, which have uniform tractions over the whole interface (as Figure 3d). These latter two models differ in that *model 4* includes the elastic modulus based upon Equation (37).

Figure 14 shows traction versus radial displacement results for the four models. The peak traction represents the traction at which the longitudinal cracks become unstable. The displacements are the average displacements for each model over the regions where the tractions are applied. The results suggest that for this example: (1) the effect of simplifying the surface geometry (*model 2* vs. *model 1*) is not significant, and (2) including the elastic modulus in the macroscopic model allows the radial response to be more accurately reproduced (*model 4* vs. *model 3*). The difference in the structural softening responses (*model* 1 vs. *model* 4) is partially due to the position of the uniform traction distribution used in *model* 4; the uniform load was distributed over the actual bonded length rather than "centering" unit surface elements with respect to the ring loads. Note that while D^e was derived for an uncracked solid, the improved results for the macroscopic model extend beyond the initial elastic response. The effect of the change in contact area with material damage is examined in a forthcoming study [39] (Cox and Yu 1998).

6. DISCUSSION AND CONCLUSIONS

For some applications where an axisymmetric reinforcing element is modeled at a scale where details of the surface structure are omitted, the effects of this surface structure should still be characterized. The radial elastic response of an interface characterization was addressed in this study. The approach presented here for determining the corresponding elastic modulus of the interface requires the homogenized traction distribution (1) to be "statically equivalent" and (2) to produce the same amount of strain energy in the constituent materials. An analytical solution of the elasticity problems associated with the "actual" and homogenized traction distributions (equivalent *problems b* and *d*) yields an analytical solution for the elastic modulus as a function of the model parameters. The solution presented assumes that the elastic strain energy stored in the matrix is much greater than that stored in the reinforcing element, but the solution is easily extended to the more general case by considering the corresponding "interior problem" of a cylinder subjected to a periodic traction. The analytical expression for D^e gives an interface characterization of the local elastic response associated with the surface structure of the reinforcing element.

While simplifying assumptions were made (e.g., axisymmetry, periodicity, homogeneous and isotropic material properties) to obtain an analytical solution, the solution does provide information on an elastic modulus for which experimental data is often lacking. Results from the solution have been applied in a specific interface model [39](Cox and Yu 1997), but several qualitative observations that may have a broader application (e.g., for rough interface surfaces with a *characteristic wave length of roughness*) can also be made.

(1) For applications where the surface structure and corresponding traction distribution scale with the diameter of the reinforcement, the elastic modulus is inversely proportional to the diameter.

(2) Even when nonzero tractions exist over the entire unit surface element, the solution justifies the use of an elastic modulus when the traction distribution is nonuniform and also indicates that the effective contact length is less than the length of the unit surface element.

(3) For the example problem considered, the elastic modulus of the interface was proportional to Young's modulus but relatively insensitive to Poisson's ratio. The prediction of longitudinal cracking by a model that idealized the interface tractions as being uniform was improved by including the elastic modulus.

(4) If one associates the change in traction distribution with contact between the surface of the reinforcing element and the matrix, the analytical solution shows the interface stiffness (a measure of "smoothness" of the surface) should increase with an increase in the effective contact area, and decrease with an increase in the characteristic length associated with the surface structure (s_r).

APPENDIX A

In this appendix, the reciprocal theorem of Betti and Rayleigh (see e.g., Sokolnikoff [31]1956) is used to show that the average radial displacement (over the interface) of *problems b* through *d* are the same when $D^e \to \infty$. It is sufficient to consider *problems b* and *d* of Figure 3 with the interface deformation of *problem d* neglected. Betti and Rayleigh's reciprocal work theorem gives the following relationship

$$\int_A t_n u_r^d \, dA = \int_A s u_r^b \, dA \qquad \text{(A-1)}$$

where the superscripts *b* and *d* denote the particular problem. Since both *s* and u_r^d are constant over the interface surface, and the interface traction distributions are "statically equivalent" (Equations (11) and (3) relate the interface tractions), the above relationship can be expressed as

$$u_r^d = \frac{1}{A}\int_A u_r^b \, dA \tag{A-2}$$

That is, the average radial displacement of the interface is independent of the radial traction distribution assuming that the traction distributions are "statically equivalent."

ACKNOWLEDGMENTS

This work was partially supported by a Young Faculty Research Initiation Grant from the Whiting School of Engineering, Johns Hopkins University and by a contract (N0024498P0366) with the Naval Facilities Engineering Service Center, Port Hueneme, CA. The authors would also like to thank Profs. Gang Bao and Leonard R. Herrmann for reviewing preliminary drafts of the paper, and for comments by a reviewer that led to improvements in the manuscript.

REFERENCES

1. Desai, C.S., M.M. Zaman, J.G. Lightner, and H.J. Siriwardane. 1984. "Thin-layer Element for Interface and Joints," *International Journal for Numerical and Analytical Methods in Geomechanics*, 8(1):19-43.
2. Desai, C.S. and B.K. Nagaraj. 1988. "Modeling for Cyclic Normal and Shear Behavior of Interfaces," *Journal of Engineering Mechanics*, ASCE, 114(7):1198-1217.
3. Chaboche, J.L., R. Girard, and A. Schaff. 1997. "Numerical Analysis of Composite Systems by Using Interphase/Interface Models," *Computational Mechanics*, 20:3-11.
4. Goodman, R.E., R.L. Taylor and T.L. Brekke. 1968. "A Model for the Mechanics of Jointed Rock," *Journal of Soil Mechanics and Foundation Division*, ASCE, 94(SM3): 637-659.
5. Herrmann, L.R. 1978. "Finite Element Analysis of Contact Problems," *Journal of Engineering Mechanics Division*, ASCE, 104(5):1043-1057.
6. Plesha, M. E., R. Ballarini, and A. Parulekar. 1989. "Constitutive Model and Finite Element Procedure for Dilatant Contact Problems", *Journal of Engineering Mechanics*, ASCE, 115(12): 2649–2668.
7. Stankowski, T., K. Runesson, and S. Sture. 1993. "Fracture and Slip of Interfaces in Cemetitious Composites. I: Characteristics," *Journal of Engineering Mechanics*, ASCE, 119(2):292-327.
8. Oden, J.T., and L. Campos. 1981. "Some New Results on Finite Element Methods for Contact Problems with Friction," In T.J.R. Hughes et al., eds., *New Concepts in Finite Element Analysis*, 44, ASME, pp. 1-9. New York: N.Y.
9. Schellekens, J.C.J., and R. de Borst. 1994. "The Application of Interface Elements and Enriched or Rate-Dependent Continua to Micro-Mechanical Analyses of Fracture in Composites," *Computational Mechanics*, 14:68-83.
10. Tsai, H.C., A.M. Arocho, and L.W. Gause. 1990. "Prediction of Fiber-matrix Interphase Properties and Their Influence on Interface Stress, Displacement and Fracture Toughness of Composite Materials," *Materials Science and Engineering*, A126:295-304.
11. Walter, M.E., G. Ravichandran, and M. Ortiz. 1997. "Computational Modeling of Damage Evolution in Unidirectional Fiber Reinforced Ceramic Matrix Composites," *Computational Mechanics*, 20:192-198.
12. Ko, Ching-Chang, D.H. Kohn, and S.J. Hollister. 1996. "Effective Anisotropic Elastic Constants of Bimaterial Interphases: Comparison Between Experimental and Analytical Techniques," *Journal of Materials Science–Materials in Medicine*, 7(2):109-117.

13. Nevard, J. and J.B. Keller. 1997. "Homogenization of Rough Boundaries and Interfaces," *SIAM Journal of Applied Mathematics*, 57(6):1660-1686.
14. Aboudi, J. 1987. "Damage in Composites Modeling of Imperfect Bonding," *Compos. Sci. Technol.*, 228:103-128.
15. Achenbach, J.D. and H. Zhu, "Effect of interphases on micro and macromechanical behavior of hexagonal-array fiber composites," *Journal of Applied Mechanics*, vol 57, 1990, pp 956-963.
16. Benveniste, Y. 1985. "The Effective Mechanical Behavior of Composite Materials with Imperfect Contact Between the Constituents," *Mech Mater.*, 4:197-208.
17. Hashin, Z. 1990. "Thermoelastic Properties of Fiber Composites with Imperfect Interfaces," *Mech. Mater.*, 8:333-348.
18. Theocaris, P.S., E.P. Sideridis, and G.C. Papanicolaou. 1985. "The Elastic Longitudinal Modulus and Poisson's Ratio of Fiber Composites," *Journal of Reinforced Plastics and Composites*, 4:396-418.
19. Jayaraman, K., K.L. Reifsnider, and R.E. Swain, 1993. "Elastic and Thermal Effects in the Interphase: Part II. Comments on Modeling Studies," *Journal of Composites Technology and Research (JCTRER)*, 151(1):3-13.
20. Goto, Y. 1971. "Cracks Formed in Concrete Around Deformed Tension Bars," *ACI Journal*, 68(4):244-251.
21. Jiang. D.H., S.P. Shah, and A.T. Andonian. 1984. "Study of the Transfer of Tension Forces by Bond," *ACI Journal*, 81(3):251-259.
22. Ozbolt, J., and R. Eligehausen. 1992. "Numerical Simulation of Cycling Bond-slip Behavior," *Bond in Concrete, Proceedings of the International Conference*, Riga, Latvia, CEB, 12.27-12.33.
23. Reinhardt, H.W., J. Blaauwendraad, and E. Vos. 1984. "Prediction of Bond Between Steel and Concrete by Numerical Analysis," *Material and Structures*, 17(100):311-320.
24. Cox, J.V. and L.R. Herrmann. 1998. "Development of A Plasticity Bond Model for Reinforced Concrete," *Mechanics of Cohesive-frictional Materials*, John Wiley and Sons, 3:155-180.
25. Cox, J.V. and L.R. Herrmann. 1998. "Validation of A Plasticity Bond Model for Reinforced Concrete," accepted for publication in *Mechanics of Cohesive-frictional Materials*, John Wiley and Sons.
24. Hutchinson, J.W., and H.M. Jensen. 1990. "Models of Fiber Debonding and Pullout in Brittle Composites with Friction," *Mechanics of Materials*, 9:139-163.
26. Parthasarathy, T.A., R.J. Kerans, and D.B. Marshall. 1994. "Analysis of the Effect of Interfacial Roughness on Fiber Debonding and Sliding in Brittle Matrix Composites," *Acta metall. mater.*, 42(11): 3773-3784.
27. Tepfers, R. 1979. "Cracking of Concrete Cover along Anchored Deformed Reinforcing Bars," *Magazine of Concrete Research*, 31(106):3-12.
28. Cox, J.V. and L.R. Herrmann. 1992. "A Plasticity Model for the Bond Between Matrix and Reinforcement," *Composites '92: Recent advances in Japan and the United States, Proceedings of the Sixth Japan-U.S. Conference on Composite Materials*. **Need page numbers.**
29. Cox, J.V. 1996. "Elastic Moduli of a Bond Model for Reinforced Concrete," In *Proceedings of the 11th ASCE engineering mechanics specialty conference*, pp. 84-87.
30. Guo, J. and J. Cox, 1998. "Modeling the Mechanical Interaction Between FRP Bars and Concrete," *Proceedings of the 13th Annual Technical Conference on Composite Materials*, American Society for Composites, September, Baltimore, Maryland.
31. Sokolnikoff, Ivan Stephen. 1956. Mathematical Theory of Elasticity, 2nd ed., McGraw-Hill.
32. Lemaitre, J. 1996. A Course on Damage Mechanics, 2nd ed., Springer-Verlag.
33. Kachanov, L.M. 1958. "Time to the Rupture Process under Creep Conditions," *IVZ. Akad Nauk*, S.S.R., Otd Tech. Nauk, (8):26-31. *– referenced for equivalent stress*

34. Lemaitre, J. 1971. "Evaluation of Dissipation and Damage in Materials Submitted to Dynamic Loading," In *Proc. I.C.M.* (1), Kyoto, Japan. *– referenced for strain equivalence*
35. Timoshenko, S., and S. Woinowsky-Krieger. 1959. Theory of Plates and Shells, 2nd ed., McGraw-Hill. **-- can't find my copy!**
36. Herrmann, L.R. and M. Tamekuni. 1965. "Horizontal Slump of Solid Propellant Motors," *American Institute of Aeronautics and Atronautics Journal*, 3(4):696-700. *-- get & ver.*
37. Kurtz, R.D. and N.J. Pagano. 1991. "Analysis of the deformation of a symmetrically-loaded fiber embedded in a matrix material," *Composites Engineering*, 1(1):13-27.
38. Malvar, L. Javier. 1992. "Bond of Reinforcement under Controlled Confinement," *ACI Materials Journal*, 89(6): 593-601.
39. Cox, J.V. and H. Yu. 1998. "Characterization of the Radial Elastic Response associated with Bond between Steel Bars and Concrete," in preparation.
40. Rots, J.G. 1988. *Computational Modeling of Concrete Fracture*, Dissertation, Department of Civil Engineering, Delft University of Technology, Delft, Netherlands.
41. Hillerborg, A., M. Modéer, and P.A. Petersson. 1976. "Analysis of Crack Formation and Crack Growth in Concrete by Means of Fracture Mechanics and Finite Elements," *Cement and Concrete Research*, 6:773-782.

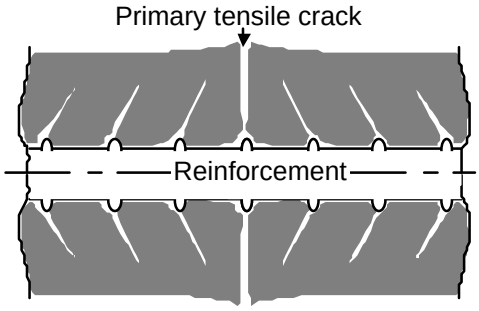

revised version

Figure 1. A reinforcing element with surface structure bridging a crack (after Goto [18]1971).

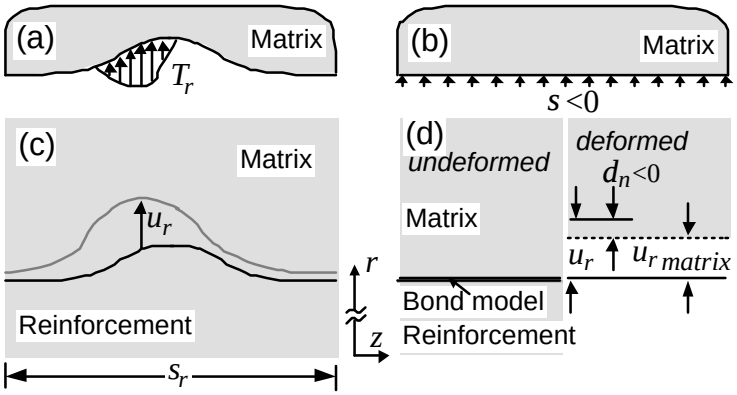

Figure 2. Bond model interface idealizations.

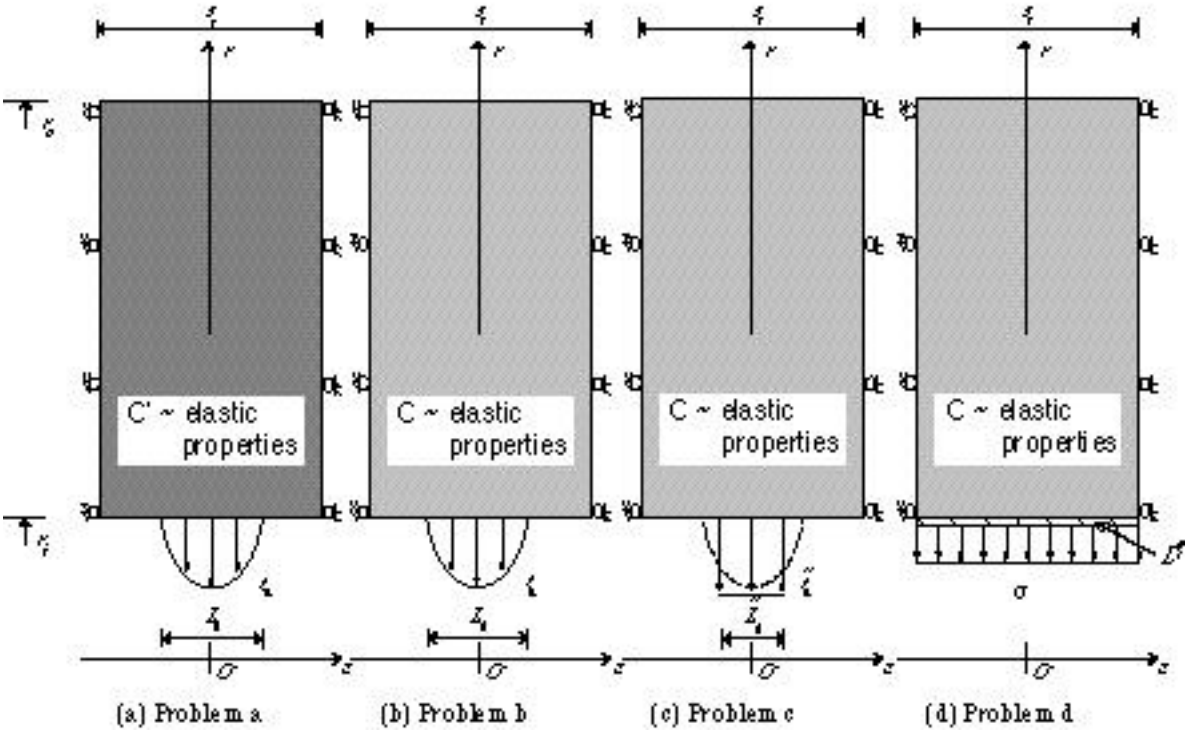

Figure 3. Idealizations for the radial response. *Revisions reduce the size of each z-axis,*

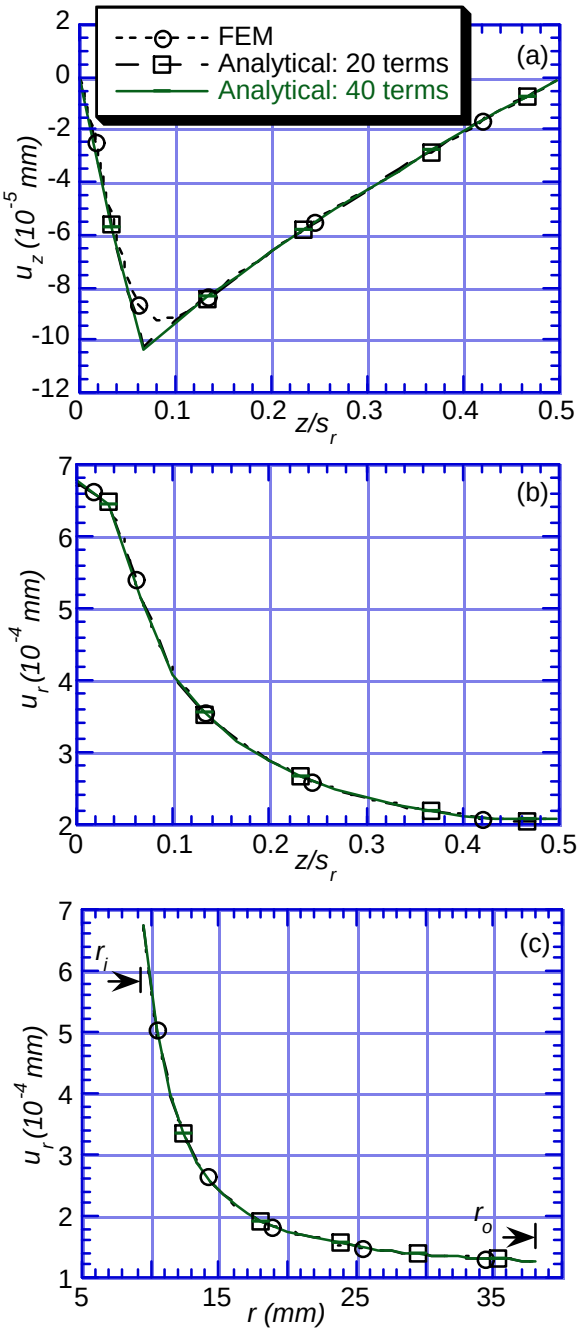

Figure 4. Analytical vs. FE solutions.

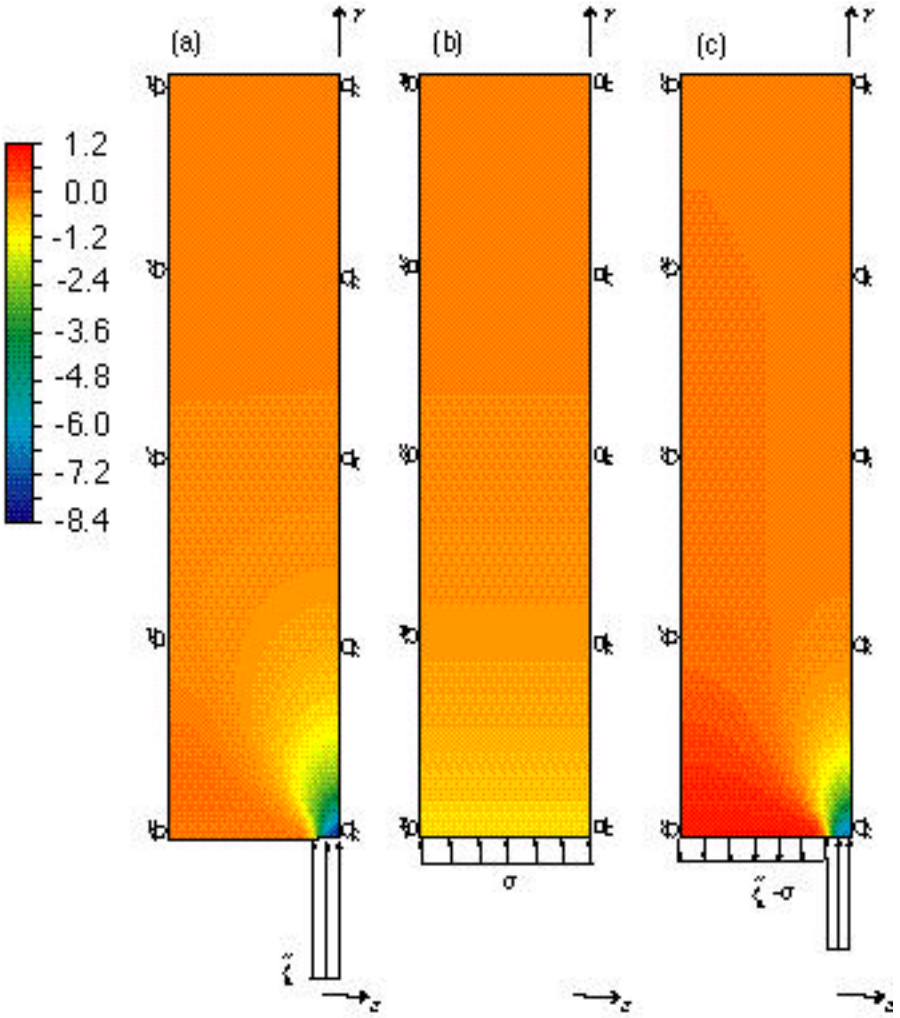

Figure 5. Finite element predictions of s_{rr} for: (a) $\tilde{t}_n$, (b) s, and (c) $\tilde{t}_n - s$.

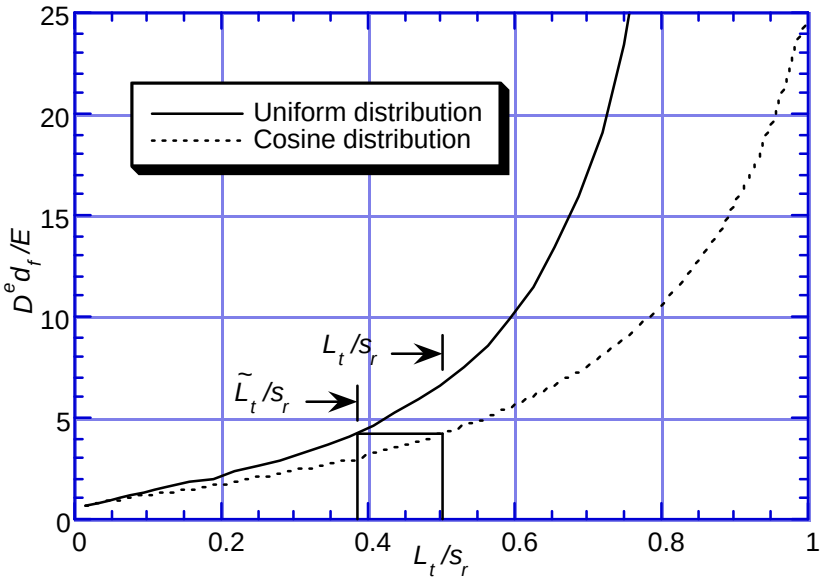

Figure 6. Variation of D^e with contact length (fixed s_r).

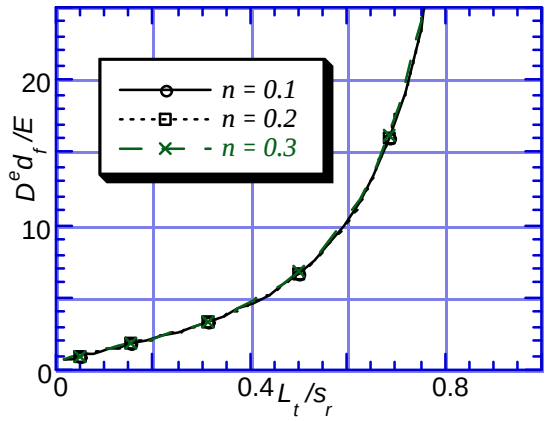

Figure 7. Sensitivity of D^e to Poisson's ratio (fixed s_r).

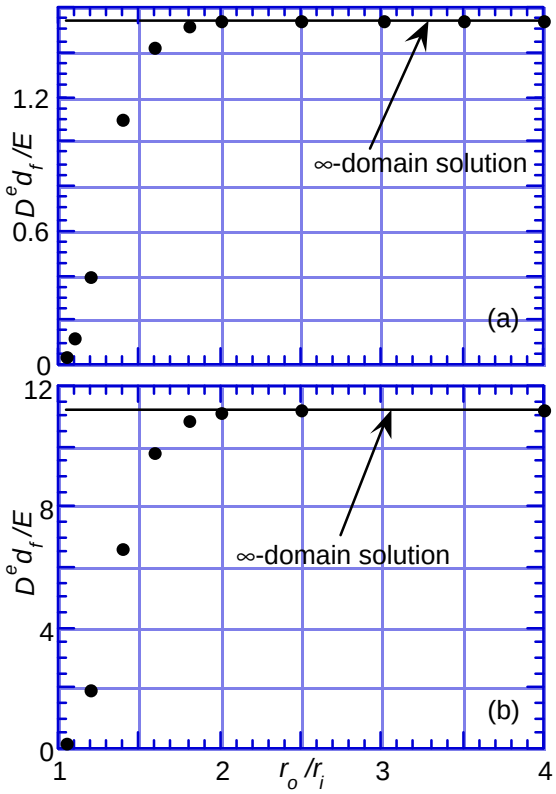

Figure 8. Finite domain solution (●) vs. ∞-domain solution: (a) L_t/s_r=0.124, and (b) L_t/s_r=5×0.124 (fixed s_r and L_t).

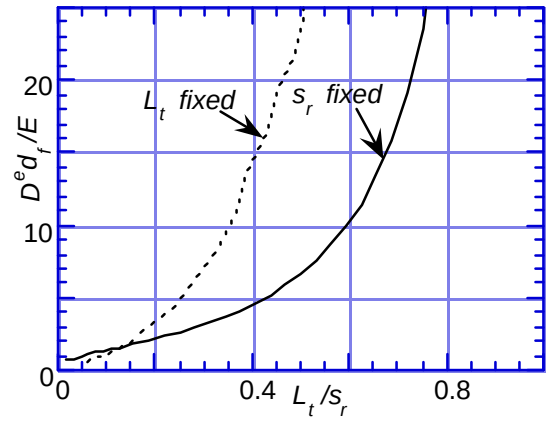

Figure 9. Variation of D^e with s_r and L_t.

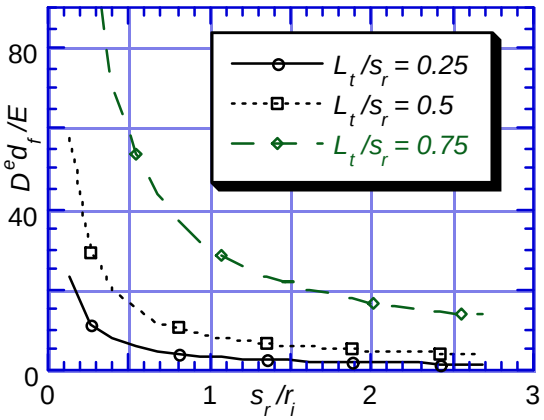

Figure 10. Variation of D^e with s_r.

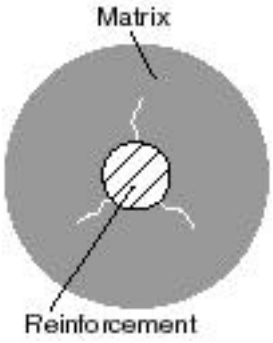

Figure 11. Longitudinal cracks in a specimen.

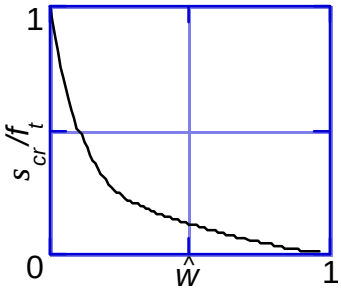

Figure 12. Traction-crack opening relationship.

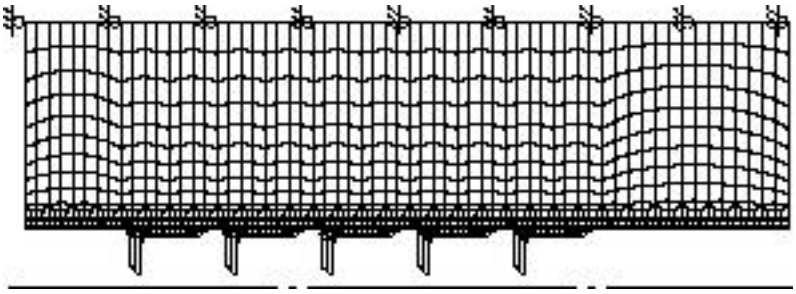

Figure 13. Model 1 of a concrete bond specimen.

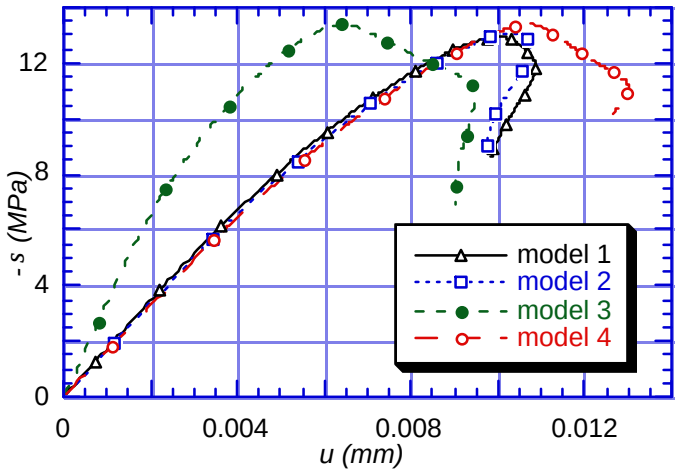

Figure 14. Traction vs. displacement for 4 specimen models.

Page: 3

[JVC1]Assumption on the relative stiffness of the matrices is not applicable to the frp bar.

Page: 3

[JVC2] Hutchinson and Jensen [24] was deleted since their analysis of misfit did not address a variation of the radius.

Page: 3

[JVC3]Do we want to say first order? Hailing didn't know how to interpret it.

Page: 6

[JVC4]Do we want to mention this?

Page: 11

[JVC5]Should we say apparent?

Page: 13

[JVC6]Correct word?